J Mol Model (2011) 17:3039–3046
DOI 10.1007/s00894-011-1014-7

ORIGINAL PAPER

Structure and electronic properties of Alq3 derivatives with electron acceptor/donor groups at the C4 positions of the quinolate ligands: a theoretical study

Joshi Laxmikanth Rao · Kotamarthi Bhanuprakash

Received: 15 November 2010 / Accepted: 8 February 2011 / Published online: 1 March 2011

Abstract The molecular structures of the ground (S_0) and first singlet excited (S_1) states of Alq3 derivatives in which pyrazolyl and 3-methylpyrazolyl groups are substituted at the C4 positions of the 8-hydroxyquinolate ligands as electron acceptors, and piperidinyl and *N*-methylpiperazinyl groups are substituted at the same positions as electron donors, have been optimized using the B3LYP/6-31G* and CIS/6-31G* methods, respectively. In order to analyze the electronic transitions in these derivatives, the frontier molecular orbital characteristics were analyzed systematically, and it was found that the highest occupied molecular orbital is localized on the A ligand while the lowest unoccupied molecular orbital is localized on the B ligand in their ground states, similar to what is seen for *mer*-Alq3. The absorption and emission spectra were evaluated at the TD-PBE0/6-31G* level, and it was observed that electron acceptor substitution causes a red-shift in the emission spectra, which is also seen experimentally. The reorganization energies were calculated at the B3LYP/6-31G* level and the results show that acceptor/donor substitution has a significant effect on the intrinsic charge mobilities of these derivatives as compared to *mer*-Alq3.

Keywords OLED · Gap energy · Optical properties · Reorganization energy

J. L. Rao (✉) · K. Bhanuprakash
Inorganic and Physical Chemistry Division, Indian Institute of Chemical Technology,
Hyderabad 500 007, India
e-mail: lkjoshiji@yahoo.com

Introduction

Organic light-emitting diodes (OLED) are currently under intense investigation due to their application in full-color flat display panels [1–4]. OLEDs are heterojunction devices in which the layers of the organic transport materials are incorporated into devices as amorphous thin films [5]. Following an initial report of the utilization of *mer*-Alq3 [6, 7] as an electron-transport material and emitting layer in OLED, derivatives of metal quinolates have become the focus of new electroluminescent material research [8–10]. Although research into the development of OLEDs in the past decade has grown rapidly, theoretical studies of the fundamental molecular properties of metaloquinolates have only been reported in the literature in recent years [11–24]. The electronic structural properties of *mer*-Alq3 can be modified by adding electron acceptor/donor groups to the peripheral ligands. In general, attaching electron donor groups to a pyridine ring causes a blue-shift in the emission, while introducing them onto phenoxide ring causes a red-shift [25–27]. Electron acceptor groups such as chloro [28] and cyano [29] show almost negligible emission shifts, while strong electron acceptors such as sulfonamide show blue-shifted emission [30]. The substitution of fluorine at different positions in the *mer*-Alq3 ligand leads to changes in emission wavelengths [31]. Recently, Hormi et al. [32] synthesized *mer*-Alq3 derivatives with electron acceptor/donor groups at the C4 positions of the 8-hydroxyquinolate ligands, and showed that emission spectra can be efficiently tuned by substitution. The present study provides a detailed theoretical study of the ground (S_0) and the first singlet excited (S_1) state

geometries of these derivatives using density functional theory (DFT) and ab initio configuration interaction with single excitation (CIS) methods, respectively. The time-dependent DFT (TDDFT) method was used to calculate the absorption and emission spectra of these derivatives, and the results are compared with the available experimental data [32]. The reorganization energies for all of the derivatives were calculated at the B3LYP/6-31G* level.

Computational details

The S_0 geometries of Alq3 derivatives (**1**–**4**) in which pyrazolyl and 3-methylpyrazolyl groups are substituted at the C4 positions of the 8-hydroxyquinolate ligands as acceptors, and piperidinyl and *N*-methylpiperazinyl groups are substituted at the same positions as donors (Fig. 1), were optimized using the DFT/B3LYP/6-31G* method in the G03 package [33]. This method has been shown to be a reliable approach for *mer*-Alq3 and its derivatives [34–40]. The S_1 geometries were optimized using the ab initio CIS approach [41], and this approach has previously been applied to *mer*-Alq3 and its derivatives [34–36, 40] and other OLED materials [42–47], yielding reliable results. The absorption and emission spectra of these derivatives were evaluated by the PBE0/6-31G* method [48] using the B3LYP/6-31G* and CIS/6-31G* optimized geometries, respectively. The reorganization energy, which is one of the most important parameters for determining the charge mobility, was calculated at the B3LYP/6-31G* level for each derivative.

Results and discussion

Ground state geometries

The ground state geometries of (**1**–**4**) are depicted in Fig. 1 [32]. The ligands in these derivatives were labeled A, B and C. The central Al atom is surrounded by the three ligands with the A- and C-pyridinate nitrogens and the B- and C-pyridinate oxygens *trans* to each other. The derivatives **1** and **2** are obtained by substituting the acceptors (namely pyrazolyl and 3-methylpyrazolyl groups) at the C4 positions of the 8-hydroxyquinolate ligands, while **3** and **4** are obtained by substituting the donors (piperidinyl and *N*-methylpiperazinyl groups, respectively) at the same position on the ligands, as shown in Fig. 1b. Selected optimized geometrical parameters of (**1**–**4**) and *mer*-Alq3 are shown in Table 1, along with the available experimental values of *mer*-Alq3 [49]. In all of the Alq3 derivatives (**1**–**4**), the Al–N bond lengths are predicted to be 0.005–0.020 Å (depending on the substitution) shorter than they are for the optimized *mer*-Alq3 (Table 1). The Al–O bond lengths are predicted to be 0.003–0.006 Å (i.e., negligibly) longer in **3** and **4**, while they are similar in **1** and **2** to the lengths seen in the optimized *mer*-Alq3

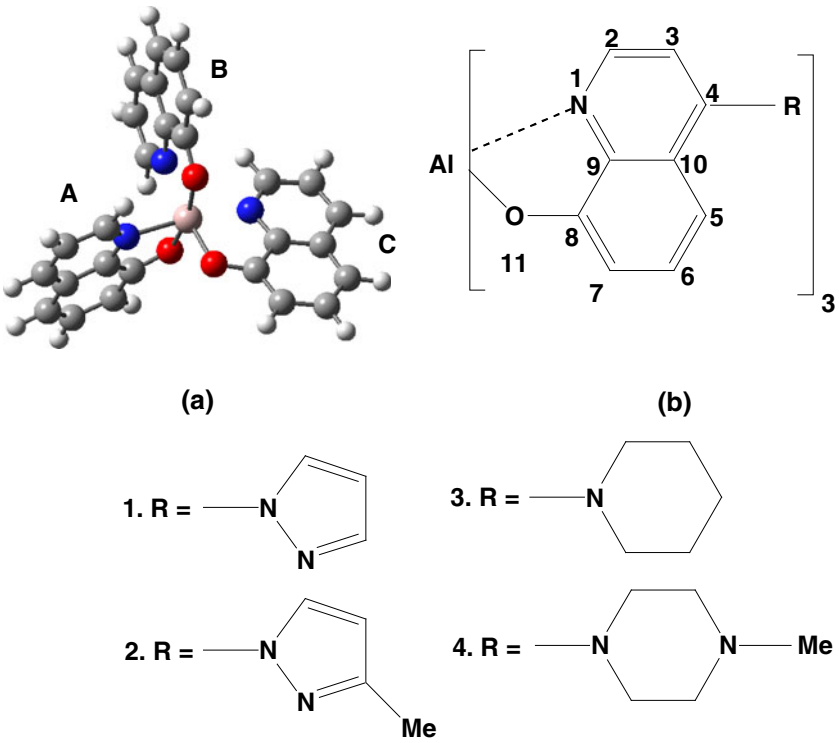

Fig. 1 **a** The geometry of *mer*-Alq3 with three quinolate ligands (A–C); **b** the ligand labeling for the Alq3 derivatives (**1**–**4**) considered for this study

Table 1 Selected optimized bond lengths (in A°), and bond angles (in degrees) of **1–4** computed at the B3LYP/6-31G* level

Parameters	Alq3	**1**	**2**	**3**	**4**	Alq3[a]
Bond lengths						
$Al–N_a$	2.084	2.079	2.078	2.073	2.074	2.050
$Al–N_b$	2.126	2.116	2.113	2.108	2.106	2.087
$Al–N_c$	2.064	2.059	2.058	2.053	2.054	2.017
$Al–O_a$	1.855	1.855	1.856	1.860	1.860	1.850
$Al–O_b$	1.881	1.881	1.882	1.886	1.887	1.860
$Al–O_c$	1.884	1.882	1.883	1.888	1.887	1.857
Bond angles						
$N_a–Al–N_c$	171.50	171.16	171.06	171.00	171.29	173.82
$N_b–Al–O_a$	172.75	172.21	172.45	172.06	171.75	171.46
$O_c–Al–O_b$	166.57	166.50	166.59	166.54	166.91	168.22

[a] Experimental data for Alq3 from [49]

(Table 1). The calculated bond lengths are slightly longer than the experimental values, which could be due to solid-state effects [50]. In the substituted ligand, the dihedral angle between the hydroxyquinolate and the acceptor is found to be ~32°, whereas it is ~19° between the hydroxyquinolate and the donor.

Frontier molecular orbitals for S_0 geometries

It is useful to examine the frontier molecular orbitals (i.e., HOMO and LUMOs) of **1–4** because the relative order of these orbitals provides a reasonable qualitative indication of the excitation properties and the hole/electron transport

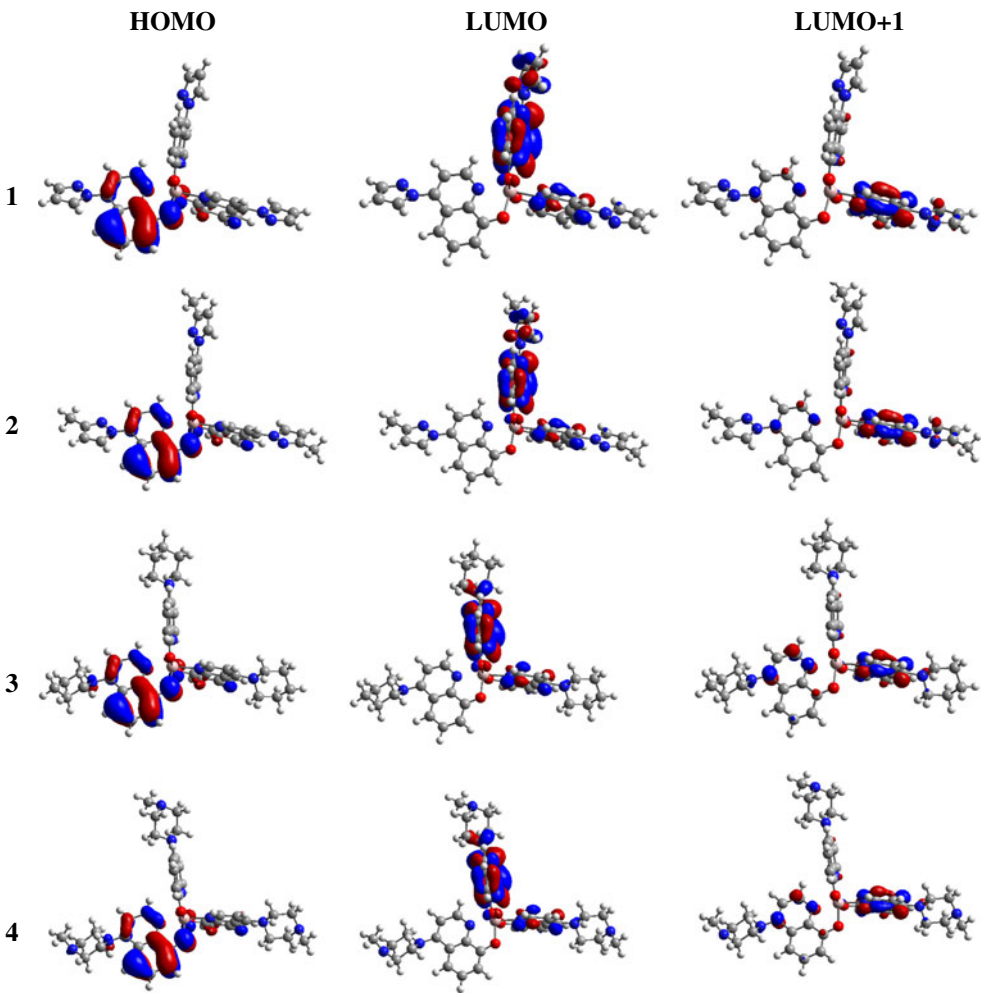

Fig. 2 Frontier molecular orbitals (FMOs) (0.05 e au^{-3}) for the ground states (S_0) of **1–4**

Table 2 HOMO, LUMO, and gap energies (E_g, in eV) of **1–4** in their ground states (S_0) computed at the PBE0//B3LYP/6-31G* level

Derivatives	HOMO	LUMO	LUMO +1	E_g	Exp[a]
Alq3	−5.261	−1.647	−1.405	3.85	3.19
1	−5.398	−1.930	−1.710	3.69	3.05
2	−5.301	−1.817	−1.596	3.71	3.06
3	−4.853	−1.108	−0.887	3.97	3.32
4	−4.914	−1.186	−0.964	3.95	3.29

[a] Experimental gap energies for Alq3 and **1–4**, from [32]

properties of **1**–**4**. It is seen in the literature that the HOMO and LUMO are mainly localized on the A ligand and B ligand, respectively, in the ground states of *mer*-Alq3 [34] and its derivatives [37, 40]. The HOMO, LUMO and LUMO+1 distribution patterns of **1**–**4** in their ground states, as obtained using the B3LYP/6-31G* method, are shown in Fig. 2. As noted in earlier reports [34, 37, 40], the HOMO and LUMOs in **3** and **4** are localized mainly localized on the A ligand and B ligand, respectively, whereas in **1** and **2** the HOMOs are localized on the A ligand and the LUMOs are localized on the B ligand and to some extent on the acceptor group (which could be due to the π-conjugation

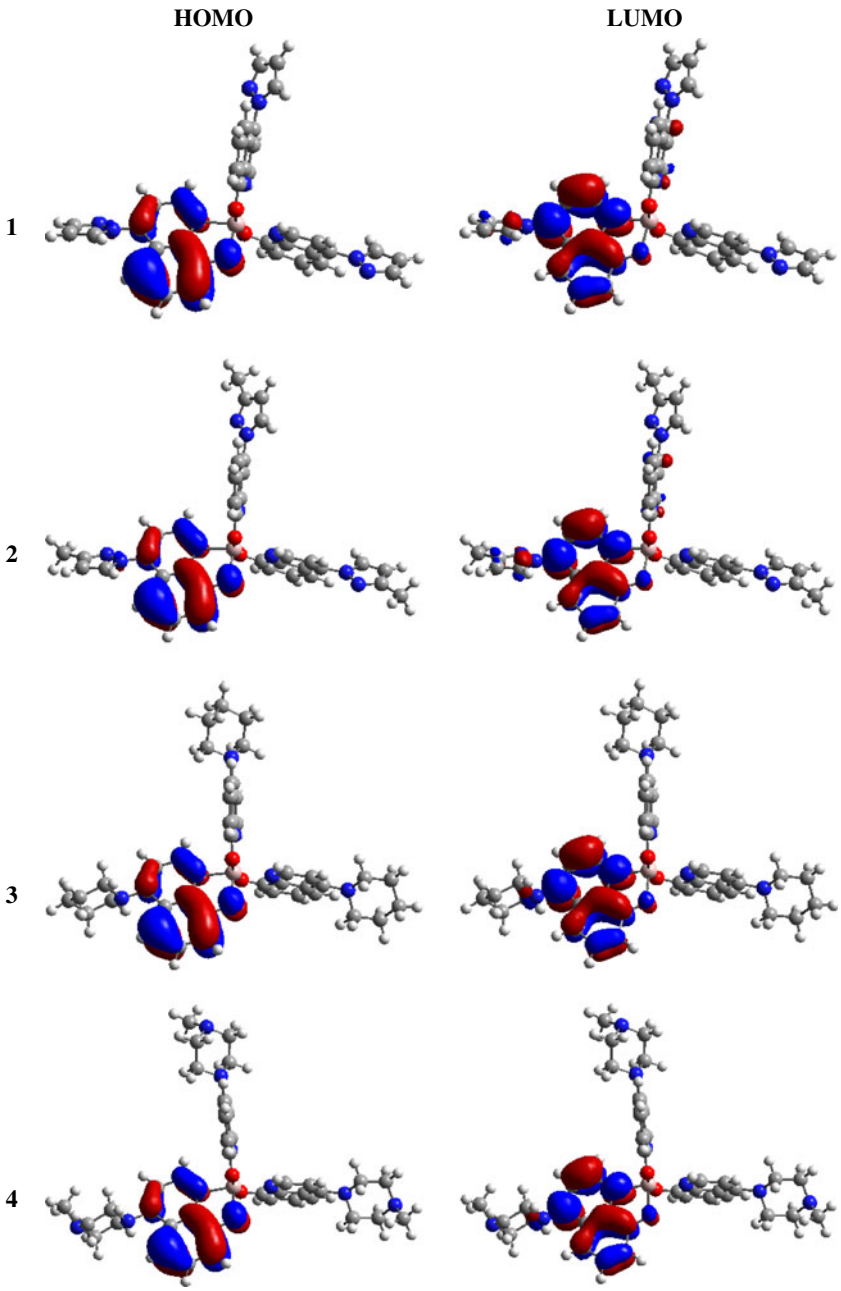

Fig. 3 Frontier molecular orbitals (FMOs) (0.05 e au^{-3}) for the excited states (S_1) of **1–4**

associated with the acceptor group) (Fig. 2). The HOMO, LUMO and LUMO+1 energies of **1**–**4** computed using TD-PBE0/6-31G*//B3LYP/6-31G* are shown in Table 2. The gap energies (E_g) were calculated as the difference between E_{HOMO} and E_{LUMO+1}, because in all of these complexes the major transitions for the absorptions are from HOMO to LUMO+1 (Table 2). It was found that the calculated E_g values for **1** (3.69 eV) and **2** (3.71 eV) are lower than the parent *mer*-Alq3 (i.e., ca. 3.85 eV), while they are higher for **3** (3.97 eV) and **4** (3.95 eV). The calculated trend in E_g values compares well with that seen experimentally [32], as reflected by their absorption spectra (Tables 2 and 4).

Frontier molecular orbitals of the first excited state (S_1) geometries

At present, the standard procedure adopted to calculate the properties of S_1 is the CIS method [41], and this has been successfully applied to *mer*-Alq3 and its derivatives [34–36, 40] and other OLED materials [42–47]. Hence, S_1 geometry optimizations for **1**–**4** were carried out by the CIS/6-31G* method using the corresponding HF/6-31G* optimized ground-state geometries. The HOMO and LUMO distribution patterns of **1**–**4** in their excited states are shown in Fig. 3. It is apparent that, for all these derivatives, the HOMO is localized on the phenoxide ring of the A ligand, while the LUMO is localized on the pyridyl ring of the A ligand (Fig. 3). The HOMO and LUMO energies of **1**–**4**, computed using the TD-PBE0/6-31G*//CIS/6-31G* method, are shown in Table 3. The calculated E_g values of **1** (3.13 eV) and **2** (3.15 eV) are lower than that of the parent Alq3 (3.22 eV), while those for **3** (3.22 eV) and **4** (3.21 eV) are comparable with that of the parent Alq3 (Table 3).

Properties of the absorption and emission spectra

Several studies have shown that TDDFT is a good predictive tool for absorption spectra; hence, TDDFT calculations were carried out for **1**–**4**. As done in previous reports [38–40, 45], various functionals (namely SVWN, BLYP, B3LYP, B3PW91, PBE0, BHandH and BHandHLYP) were used to determine the functional that gave the best performance in predicting the maximum absorption (λ_{max}) of **1** and **3** using the B3LYP/6-31G* optimized geometry, and the results are tabulated in Table 4. The λ_{max} values vary significantly depending on the functionals employed (Table 4). The performance of the local density approximation (SVWN) and pure gradient-corrected functionals (BLYP) was found to be poor when compared to the hybrid functionals (B3LYP, B3PW91, PBE0, BHandH, and BHandHLYP). Among all of the functionals, the PBE0 method was found to be the most reliable for predicting the λ_{max} values of **1** and **3** (Table 4). To investigate the effect of extending the basis sets on the absorption of **1** and **3**, calculations were carried out using the PBE0 method and different basis sets, namely 6-31+G*, 6-31G and 3-21+G**, and the results indicate that the basis set has a negligible effect on the absorption (Table 4). Among all of the functionals used to calculate the absorption spectra, the TD-PBE0/6-31G* results for **1** (434 nm) and **3** (397 nm) give the closest agreement with experimentally obtained spectra (Table 4). Hence, the PBE0 functional was chosen to calculate the absorption and emission spectra of **1**–**4** using the B3LYP/6-31G* and CIS/6-31G* optimized geometries, respectively, and the results are summarized in Table 5 along with experimental absorption and emission data [32]. In all of these complexes, the major

Table 3 HOMO, LUMO, and gap energies (E_g) (in eVs) of **1**–**4** in their first excited states (S_1), computed at the PBE0//CIS/6-31G* level

Derivatives	HOMO	LUMO	E_g
Alq3	−4.873	−1.649	3.22
1	−5.047	−1.915	3.13
2	−4.959	−1.807	3.15
3	−4.577	−1.358	3.22
4	−4.636	−1.426	3.21

Table 4 Absorption wavelengths (λ_{max}, in nm) computed at various levels of DFT theory using the B3LYP/6-31G* optimized geometry for **1** and **3**. The effect of the basis set is also shown using TD-PBE0

Method	6-31G*	6-31G	6-31+G*	3-21G*
Al derivative **1**				
SVWN	676			
BLYP	669			
B3LYP	465			
B3PW91	466			
PBE1PBE	434	442	439	437
BHandH	364			
BHandHLYP	364			
Exp[a]	407			
Al derivative **3**				
SVWN	676			
BLYP	669			
B3LYP	465			
B3PW91	466			
PBE1PBE	397	405	404	400
BHandH	341			
BHandHLYP	340			
Exp[a]	374			

[a] Experimental λ_{abs} for **1** and **3**, from [32]

Table 5 Calculated absorption (λ_{abs}) and emission (λ_{emi}) wavelengths (in nms) of **1–4** at the TD-PBE0/6-31G* level

Derivatives	Absorption				Emission			
	Major transitions[a]	λ_{abs}	f[b]	λ_{abs}[c]	Major transitions	λ_{emi}	f[b]	λ_{emi}[c]
Alq3[c]				389				512
1	H→L+1	426	0.1551	407	H→L	536	0.0776	535
2	H→L+1	423	0.1753	406	H→L	531	0.0872	534
3	H→L+1	391	0.1686	374	H→L	523	0.0678	477
4	H→L+1	393	0.1755	377	H→L	525	0.0676	485

[a] *H* and *L* are HOMO and LUMO, respectively

[b] *f* is the oscillator strength

[c] Experimental λ_{abs} and λ_{emi} for *mer*-Alq3 and **1–4** from [32]

transitions for absorption were from HOMO to LUMO+1, while for emission they were from HOMO to LUMO (Table 5). In the case of absorption spectra, the calculated absorption values are in good agreement with the experimental ones [32], with deviations of ~16–19 nm depending on the substitution at the C4 position of 8-hydroxyquinolate ligand (Table 5). Substituting an acceptor at the C4 position of the quinolate ligand (i.e., in **1** and **2**) leads to a red shift of ~16–21 nm in the emission spectrum compared to the parent *mer*-Alq3, which is similar to that seen experimentally [32].

Reorganization energies

The charge transfer rate can be defined using Marcus theory [51]:

$$K_{et} = (4\pi^2/h)H_{da}{}^2(4\pi\lambda kT)^{-1/2}\exp(-\lambda/4kT) \quad (1)$$

Here, H_{da} is the charge transfer integral/coupling matrix element between neighboring molecules, λ is the reorganization energy, k is the Boltzmann constant and T is the temperature. The two major parameters that determine transfer rates and ultimately the charge mobility are H_{da} and λ, which should be maximized and minimized, respectively, to achieve significant charge transport. Evaluating H_{da} would require the relative positions of the molecules in the solid state, as it is related to the splitting of the energies of the frontier orbitals of the interacting molecules. On the other hand, electron or hole transport is predicted from the electron (λ_{ele}) or hole (λ_{hole}) reorganization energy, and the values for these parameters generally show good agreement with experimental observations [51–60]. Crystal data are required in order to calculate the charge transfer integrals, and these data are not available, so we calculated only the reorganization energy (the other important mobility parameter), for all of these derivatives. The hole and electron reorganization energies are calculated via the following equations:

$$\text{For hole transport}: \quad \lambda_{hole} = \lambda_1 + \lambda_2 \quad (2)$$

$$\text{For electron transport}: \quad \lambda_{ele} = \lambda_3 + \lambda_4 \quad (3)$$

where $\lambda_1(\lambda_3)$ is the energy required to reorganize the neutral geometry into that of the cation(anion) upon the removal(addition) of an electron along the cation(anion)-state potential energy surface, and $\lambda_2(\lambda_4)$ is the energy required to reorganize the obtained cation(anion) geometry back into the neutral geometry upon the addition(removal) of an electron along the ground-state potential energy surface.

The hole/electron reorganization energies for *mer*-Alq3 [47] and its derivatives [38, 39, 61–63] were previously calculated at the B3LYP/6-31G* level. Hence, reorganization energy calculations were carried out for **1–4** using the same methodology, and the results were compared with *mer*-Alq3 (Table 6). In general, acceptor substitution favors n-channel materials, while donor substitution favors p-channel materials [64]. From Table 6, it is clear that the λ_{hole} values of all of the derivatives are higher than that of the parent *mer*-Alq3 (ca. 0.242 eV [47]). The introduction of a donor group onto the ligand increases the λ_{ele} values of **3** (0.371 eV) and **4** (0.380 eV), while the introduction of an acceptor group onto the ligand lowers the λ_{ele} values of **1** (0.237 eV) and **2** (0.247 eV) when compared with the λ_{ele} values (0.276 eV [47]) of *mer*-Alq3. From these results, it is clear that donor/acceptor substitution has a significant effect on the intrinsic charge mobility when compared to that of *mer*-Alq3.

Conclusions

The S_0 of Alq3 derivatives in which electron acceptor/donor groups are substituted at the C4 positions of the 8-hydroxyquinolate ligands have been optimized using the DFT/B3LYP/6-31G* method. From frontier molecular

Table 6 Calculated hole (λ_{hole}) and electron (λ_{ele}) reorganization energies (in eV) of **1–4** calculated at the B3LYP/6-31G* level

Derivatives	λ_{hole}	λ_{ele}
Alq3[a]	0.242	0.276
1	0.264	0.237
2	0.262	0.247
3	0.327	0.371
4	0.336	0.380

[a] Alq3 data from [47]

orbital analysis, it is apparent that the HOMOs and LUMOs are localized mainly on the A ligand and B ligand, respectively, in these derivatives—similar to the parent *mer*-Alq3 and its derivatives. The calculated trend in the gap energies is in good agreement with that observed experimentally. The CIS/6-31G* method was used to obtain the S_1 states. The calculations of absorption and emission spectra were carried out using the TD-PBE0/6-31G* method, and the results were found to be comparable with those found experimentally. Acceptor substitution causes a similar red-shift in the calculated emission spectra to that seen experimentally. The reorganization energies were calculated at the B3LYP/6-31G* level, and the results show that donor/acceptor substitution has a significant effect on the intrinsic charge mobility as compared to *mer*-Alq3. Thus, theoretical studies of the structural, electronic and charge-transport properties of such complexes may be useful when designing efficient emitters for use in OLEDs.

Acknowledgments The authors thank the Director of the Indian Institute of Chemical Technology and the Head of the Inorganic Chemistry division, Indian Institute of Chemical Technology, for their constant encouragement in this work.

References

1. Williams EL, Haavisto K, Li J, Jabbour GE (2007) Adv Mater 19:197–202
2. Sun Y, Giebink NC, Kanno H, Ma B, Thompson ME, Forrest SR (2006) Nature 440:908–912
3. Yeh SJ, Chen HY, Wu MF, Chan LH, Chiang CL, Yeh HC, Chen CT, Lee JH (2006) Org Electron 7:137–143
4. Choi JH, Kim KH, Choi SJ, Lee HH (2006) Nanotechnology 17:2246–2249
5. Chen CH, Shi J (1998) Coord Chem Rev 171:161–174
6. Tang CW, van Slyke SA (1987) Appl Phys Lett 51:913–915
7. Tang CW, van Slyke SA, Chen CH (1989) J Appl Phys 65:3610–3616
8. Hamada Y (1997) IEEE Trans Electron Devices 44:1208–1217
9. Van Slyke SA, Chen CH, Tang CW (1996) Appl Phys Lett 69:2160–2162
10. Curioni A, Boero M, Andreoni W (1998) Chem Phys Lett 294:263–271
11. Curioni A, Andreoni W (1999) J Am Chem Soc 121:8216–8220
12. Curioni A, Andreoni W, Treusch R, Himpsel RF, Haskal E, Seidler P, Kakar S, van Buuren T, Terminello L (1998) J Appl Phys Lett 72:1575–1577
13. Johansson N, Osada T, Stafstrom S, Salaneck WR, Parente V, dos Santos DA, Crispin X, Bredas JL (1999) J Chem Phys 111:2157–2163
14. Halls MD, Aroca R (1998) Can J Chem 76:1730–1736
15. Kushto GP, Iizumi Y, Kido J, Kafafi ZH (2000) J Phys Chem A 104:3670–3680
16. Amati M, Lelj F (2002) Chem Phys Lett 363:451–457
17. Burrows PE, Gu G, Bulovic V, Shen Z, Forrest SR, Thomson ME (1997) IEEE Trans Electron Devices 44:1188–1203
18. Su Z, Cheng H, Gao H, Sun S, Chu B, Wang R, Wang Y (2000) Gaodeng Xuexiao Huaxue Xuebao 21:1416–1421
19. Anderson S, Weaver MS, Hudson AJ (2000) Synth Met 111–112:459–463
20. Martin RL, Kress JD, Campbell IH, Smith DL (2000) Phys Rev B 61:15804–15811
21. Stampor W, Kalinowski J, Marconi G, Di Marco P, Fattori V, Giro G (1998) Chem Phys Lett 283:373–380
22. Bacon AD, Zerner MC (1979) Theor Chim Acta 53:21–54
23. Zhang RQ, Lee CS, Lee ST (2000) Chem Phys Lett 326:413–420
24. Sugimoto M, Sakaki S, Sakanoue K, Newton MD (2001) J Appl Phys 90:6092–6097
25. Yu J, Shen Z, Sakuratani Y, Suzuki H, Tokita M, Miyata S (1999) Jpn J Appl Phys 38:6762–6763
26. Sapochak LS, Padmaperuma A, Washton N, Endrino F, Schmett GT, Marshall J, Fogarty D, Burrows PE, Forrest SR (2001) J Am Chem Soc 123:6300–6307
27. Montes VA, Pohl R, Shinar J, Anzenbacher P Jr (2006) Chem Eur J 12:4523–4535
28. Jang H, Do LM, Kim Y, Kim JG, Zyung T, Do Y (2001) Synth Met 121:1669–1670
29. Burrows PE, Shen Z, Bulovic V, McCarty DM, Forrest SR, Cronin JA, Thompson ME (1996) J Appl Phys 79:7991–8006
30. Hopkins TA, Meerholz K, Shaheen S, Anderson ML, Schmidt A, Kippelen B, Padias AB, Hall HK Jr, Peyghambarian N, Armstrong NR (1996) Chem Mater 8:344–351
31. Shi YW, Shi MM, Huang JC, Chen HZ, Wang M, Liu XD, Ma YG, Xu H, Yang B (2006) Chem Commun 18:1941–1943
32. Omar WAE, Haverinen H, Hormi OEO (2009) Tetrahedron 65:9707–9712
33. Frisch MJ, Trucks GW, Schlegel HB, Scuseria GE, Robb MA, Cheeseman JR, Montgomery JA Jr, Vreven T, Kudin KN, Burant JC, Millam JM, Iyengar, SS, Tomasi J, Barone V, Mennucci B, Cossi M, Scalmani G, Rega N, Petersson GA, Nakatsuji H, Hada M, Ehara M, Toyota K, Fukuda R, Hasegawa J, Ishida M, Nakajima T, Honda Y, Kitao O, Nakai H, Klene M, Li X, Knox JE, Hratchian HP, Cross JB, Bakken V, Adamo C, Jaramillo J, Gomperts R, Stratmann RE, Yazyev O, Austin AJ, Cammi R, Pomelli C, Ochterski JW, Ayala PY, Morokuma K, Voth GA, Salvador P, Dannenberg JJ, Zakrzewski VG, Dapprich S, Daniels AD, Strain MC, Farkas O, Malick DK, Rabuck AD, Raghavachari K, Foresman, JB, Ortiz JV, Cui Q, Baboul AG, Clifford S, Cioslowski J, Stefanov BB, Liu G, Liashenko A, Piskorz P, Komaromi I, Martin RL, Fox DJ, Keith T, Al-Laham MA, Peng CY, Nanayakkara A, Challacombe M, Gill PMW, Johnson B, Chen W, Wong MW, Gonzalez C, Pople JA (2004) Gaussian 03, revision D. 01. Gaussian Inc., Wallingford
34. Zhang J, Frenking G (2004) J Phys Chem A 108:10296–10301
35. Zhang J, Frenking G (2004) Chem Phys Lett 394:120–125
36. Gahungu G, Zhang J (2005) J Phys Chem B 109:17762–17767
37. Irfan A, Cui R, Zhang J (2008) J Mol Struct THEOCHEM 850:79–83
38. Irfan A, Cui R, Zhang J (2009) Theor Chem Acc 122:275–281
39. Irfan A, Zhang (2009) J Theor Chem Acc 124:339–344
40. Rao JL, Bhanuprakash K Structure and electronic properties of Tris (4-hydroxy-1,5-naphthyridinato) aluminum (AlND3) and its methyl derivatives: A Theoretical Study, Theor Chem Acc (in press)
41. Halls MD, Schlegel HB (2001) Chem Mater 13:2632–2640
42. Gahungu G, Zhang J (2005) Chem Phys Lett 410:302–306
43. Yang Z, Yang S, Zhang J (2007) J Phys Chem A 111:6354–6360
44. Hu B, Gahungu G, Zhang J (2007) J Phys Chem A 111:4965–4973
45. Teng YL, Kan YH, Su ZM, Liao Y, Yang SY, Wang RS (2007) Theor Chem Acc 117:1–5
46. Sun M, Niu B, Zhang J (2008) J Mol Struct THEOCHEM 862:85–91
47. Lin BC, Cheng CP, You ZQ, Hsu CP (2005) J Am Chem Soc 127:66–67

48. Adamo C, Barone V (1999) J Chem Phys 110:6158–6170
49. Brinkmann M, Gadret G, Muccini M, Taliani C, Masciocchi N, Sironi A (2000) J Am Chem Soc 122:5147–5157
50. Jonas V, Frenking G, Reetz MT (1994) J Am Chem Soc 116:8741–8753
51. Marcus RA (1956) J Chem Phys 24:966–978
52. Lin BC, Cheng CP, Lao ZPM (2003) J Phys Chem A 107:5241–5251
53. Cornil J, Lemaur V, Calbert JP, Bredas JL (2002) Adv Mater 14:726–729
54. Deng WQ, Goddard WA III (2004) J Phys Chem B 108:8614–8621
55. Pan JH, Chou YM, Chiu HL, Wang BC (2007) J Phys Org Chem 20:743–753
56. Curioni A, Boero M, Andreoni W (1998) Chem Phys Lett 294:263–271
57. Wang I, Estelle BA, Olivier S, Alain I, Baldeck PL (2002) J Opt A Pure Appl Opt 4:S258–S260
58. Bredas JL, Beljonne D, Coropceanu V, Cornil J (2004) Chem Rev 104:4971–5004
59. Raghunath P, Reddy AM, Gouri C, Bhanuprakash K, Rao VJ (2006) J Phys Chem A 110:1152–1162
60. Yang L, Feng JK, Ren AM (2007) J Mol Struct THEOCHEM 816:161–121
61. Liu YL, Feng JK, Ren AM (2007) J Phys Org Chem 20:600–609
62. Wang W, Dong S, Yin S, Yang J, Lu J (2008) J Mol Struct THEOCHEM 867:116–121
63. Fang XH, Hao YY, Han PD, Xu BS (2009) J Mol Struct THEOCHEM 896:44–48
64. Zaumseil J, Sirringhaus H (2007) Chem Rev 107:1296–1323